Cerebral Cortex Advance Access published May 26, 2014

Cerebral Cortex
doi:10.1093/cercor/bhu110

Observed, Executed, and Imagined Action Representations can be Decoded From Ventral and Dorsal Areas

Flavia Filimon[1,2,†], Cory A. Rieth[3,†], Martin I. Sereno[4] and Garrison W. Cottrell[5]

[1]Adaptive Behavior and Cognition, Max Planck Institute for Human Development, Berlin, Germany, [2]Berlin School of Mind and Brain, Humboldt-Universität zu Berlin, Germany, [3]Department of Psychology, University of California, San Diego, USA, [4]Birkbeck/UCL Centre for NeuroImaging, London, UK and [5]Department of Computer Science and Engineering, University of California, San Diego, USA

Address correspondence to Flavia Filimon, Adaptive Behavior and Cognition, Max Planck Institute for Human Development, Berlin 14195, Germany. Email: flavia.filimon@gmail.com
[†]These authors shared first authorship.

Previous functional magnetic resonance imaging (fMRI) research on action observation has emphasized the role of putative mirror neuron areas such as Broca's area, ventral premotor cortex, and the inferior parietal lobule. However, recent evidence suggests action observation involves many distributed cortical regions, including dorsal premotor and superior parietal cortex. How these different regions relate to traditional mirror neuron areas, and whether traditional mirror neuron areas play a special role in action representation, is unclear. Here we use multi-voxel pattern analysis (MVPA) to show that action representations, including observation, imagery, and execution of reaching movements: (1) are distributed across both dorsal (superior) and ventral (inferior) premotor and parietal areas; (2) can be decoded from areas that are jointly activated by observation, execution, and imagery of reaching movements, even in cases of equal-amplitude blood oxygen level-dependent (BOLD) responses; and (3) can be equally accurately classified from either posterior parietal or frontal (premotor and inferior frontal) regions. These results challenge the presumed dominance of traditional mirror neuron areas such as Broca's area in action observation and action representation more generally. Unlike traditional univariate fMRI analyses, MVPA was able to discriminate between imagined and observed movements from previously indistinguishable BOLD activations in commonly activated regions, suggesting finer-grained distributed patterns of activation.

Keywords: action observation network, human fMRI, mirror neurons, MVPA, reaching

Introduction

Recent neuroimaging studies have shown several premotor and posterior parietal cortical areas to be active during both observation and execution of various hand movements (for reviews, see Rizzolatti and Fabbri-Destro 2008; Molenberghs et al. 2009; Caspers et al. 2010; Rizzolatti and Sinigaglia 2010; Molenberghs et al. 2012). It has generally been assumed that an overlap between execution and observation of action is due to the activity of mirror neurons, which are hypothesized to map observed actions onto a subset of the same motor representations involved in generating such motor acts (Caspers et al. 2010; Fogassi and Ferrari 2011). Mirror neurons were initially found in macaque ventral premotor area F5 for observation and execution of hand or mouth goal-directed movements, such as grasping or manipulating objects (di Pellegrino et al. 1992; Gallese et al. 1996; Rizzolatti et al. 1996; Fogassi and Ferrari 2011). Similar response properties were subsequently reported in inferior parietal lobule (IPL) neurons (Fogassi et al. 2005). As a result of these findings, researchers have called the IPL-F5 pathway the "mirror neuron system" (MNS) (Rizzolatti and Sinigaglia 2010).

However, recent neurophysiological and imaging evidence in macaques has increasingly shown that neurons outside the IPL-F5 circuit also represent both observed and executed actions, including neurons in dorsal premotor cortex (PMd, Cisek and Kalaska 2002; Raos et al. 2007), the supplementary motor area (SMA; Mukamel et al. 2010), primary motor cortex (M1; Raos et al. 2004a; Tkach et al. 2007; Dushanova and Donoghue. 2010; Vigneswaran et al. 2013), and superior parietal, medial parietal, intraparietal, and parieto-occipital cortices (Evangeliou et al. 2009; Savaki 2010).

Human functional neuroimaging studies have likewise demonstrated an overlap between motor observation, execution, and even motor imagery in PMd, SMA, M1, primary somatosensory cortex (S1), the superior parietal lobule (SPL), the intraparietal sulcus (IPS), and the precuneus (medial parietal cortex), in addition to the classical mirror neuron areas, that is, ventral premotor cortex (PMv), the inferior frontal gyrus (IFG, which includes Broca's area, the putative human homolog of macaque F5), and the IPL (including angular gyrus and supramarginal gyrus [SMG]) (Filimon et al. 2007; Keysers and Gazzola 2009; for reviews, see Grèzes and Decety 2001; Molenberghs et al. 2009, 2012; Caspers et al. 2010). In fact, transcranial magnetic stimulation (TMS) studies in M1 show that observation of hand actions leads to an enhancement of motor evoked potential amplitudes in distal muscles (Fadiga et al. 1995). This has been interpreted as evidence of MNS involvement, even though original mirror neuron research in macaques explicitly ruled out an M1 involvement or Electromyogram (EMG) activation during the firing of premotor mirror neurons (Hickok 2009). Other studies have reported an absence of muscle/EMG activity during action observation despite M1 activation (Raos et al. 2004a) or suppression of spinal cord activity during action observation (Stamos et al. 2010).

The wider network of sensorimotor regions involved in action observation and execution is sometimes referred to as the action observation network (AON), of which the ventrally located IFG/PMv–IPL MNS is thought to be a subcomponent (Grafton 2009; Cross et al. 2009; Ramsey and Hamilton 2010). However, the functional differences and relationship between the ventral MNS and the wider AON are unclear. A recent meta-analysis of 125 neuroimaging studies found consistent involvement of not only the IFG, PMv and IPL, but also PMd and SPL, in both observation and execution (Molenberghs et al. 2012). Despite joint involvement of classical mirror neuron

areas and wider AON regions in such tasks, ventral activations in the PMv and IPL are generally interpreted as being due to mirror neuron activity and are ascribed to the MNS, while activations outside these traditional MNS regions are assigned a nonmirror-neuron function or alternate mechanisms (for reviews as well as critiques of studies making such a distinction, see Grafton 2009; Cross et al. 2009; Keysers and Gazzola 2009; Hickok 2009; Molenberghs et al. 2009; Decety 2010; Rizzolatti and Sinigaglia 2010; Savaki 2010; Baird et al. 2011). However, whether the distinction between traditional MNS regions and the wider AON network is actually justified is unknown, given that both ventral and dorsal parieto-frontal areas participate in action observation and execution. Initial macaque studies had found that ventral premotor mirror neurons only responded to observation and execution of object-directed (interactive) actions such as grasping, placing, and manipulation, but not to observation of meaningless gestures such as lifting the arms, waving the hands, mimicking grasping in the absence of an object, or movements performed with tools (Gallese et al. 1996). This has led to the assumption that mirror neurons for action are primarily driven by, or even require, goal-directed hand–object (or mouth–object) interactions. However, recent macaque recordings in mirror neurons have challenged these assumptions: the presence of an object is not required (Kraskov et al. 2009); actions performed with tools do drive mirror neurons (Ferrari et al. 2005), and observation of meaningless, nongoal-directed forelimb movements is also effective (Raos et al. 2014).

Importantly, different sensorimotor areas in premotor cortex respond preferentially to different movements, suggesting that observation of different movements needs to be tested in different areas. For instance, PMd (F2) neurons respond during reaching even without grasping (for a review, see Filimon 2010). In fact, observation, execution, and imagery of reaching preferentially activate dorsal, rather than ventral, premotor areas, as well as the SPL, in addition to intraparietal and inferior parietal areas (Filimon et al. 2007). A common involvement of superior parietal areas for reaching-to-grasp and observation of reaching-to-grasp has also been documented in macaques (Evangeliou et al. 2009).

This suggests a rough somatotopic organization of both action observation and execution networks, with local hand movements preferentially activating more ventrally located areas, and arm movements such as reaching preferentially activating more dorsally located areas (with a degree of overlap between the two). Buccino et al. (2001) observed a somatotopic organization for observation of mouth, hand, and foot movements in premotor and posterior parietal cortex (PPC). Similarly, Sakreida et al. (2005) found that observed distal (e.g., finger, mouth), proximal (e.g., elbow, wrist), and axial (shoulder, trunk) movements are organized roughly somatotopically in premotor cortex (although see Morin and Grèzes 2008, who suggest that the somatotopic organization may be task-dependent and idiosyncratic). Another possibility is that the functional organization is based on ethologically-relevant (e.g., defensive; feeding) actions (Kaas et al. 2011; Kaas 2012) or on different types of actions irrespective of the effector (Jastorff et al. 2010; Abdollahi et al. 2012; note, however, that these studies have found large overlaps between activations for observation of such actions, suggesting the organization is neither purely action-specific nor purely effector-specific; see also Heed et al. 2011).

This functional organization of observed actions raises the possibility of *multiple* mirror neuron networks which are activated by different effector movements or types of actions, and which serve different functions depending on their anatomical location. Such an organization argues against a single inferior/ventral parieto-frontal MNS for actions. Note that this is separate from the question of whether additional mirror neuron networks exist for empathy, song recognition, and other processes not involving limb movements (Rizzolatti and Sinigaglia 2010). The existence of multiple parieto-frontal mirror neuron networks for different actions or movements is compatible with the view that mirror neurons are simply sensorimotor association cells that are involved in action selection and sensory-to-motor mappings, without assuming that they are necessary for action understanding per se (Hickok 2009; Hickok and Hauser 2010). This also raises the question of whether matching of observed and executed actions is achieved by mirror neurons or by a more general mechanism present in various types of sensorimotor neurons. For instance, it has been argued that mental simulation, which entails simulating the observed action by activating one's own motor system, is present in sensorimotor neurons in general, and not just in mirror neurons (Grafton 2009; Savaki 2010).

The widespread overlapping activations for execution, observation, and imagery of movements, together with the simulation theory of action matching (Jeannerod 1994; Grafton 2009; Savaki 2010), additionally raise the question of how we are able to keep our own actions (executed or imagined) apart from observed actions performed by others. Can these conditions be distinguished based on different patterns of activation within commonly activated areas, or are they only distinguished based on different areas of activation, for example, primary motor and sensory areas, or inhibitory mechanisms within or downstream of such areas?

Here, we investigate the fine-grained representation of action-related information across the entire premotor cortex and PPC. We use multi-voxel pattern analysis (MVPA) to investigate the spatial distribution of action-related cortical representations of observation, execution, and mental simulation (imagery) of reaching movements, to determine where, outside of primary sensory and motor areas, voxels with the most differentiating activity are concentrated. Using MVPA, we ask if the most informative voxels are concentrated within (1) traditional ventral mirror neuron areas, such as PMv/Broca's area and IPL; (2) dorsal parieto-frontal action observation areas; or (3) are distributed across multiple regions within both ventral and dorsal premotor cortex and PPC.

If traditional ventral mirror neuron areas are the basis for observation–execution matching, then MNS areas should confuse these conditions more than non-MNS areas. In this case, the most discriminating voxels should be clustered outside the MNS, even if some differential activation in the traditional MNS is to be expected, since individual mirror neurons discharge more strongly to executed than observed actions (di Pellegrino et al. 1992). Indeed, if simulation underlies observation and execution matching, then the traditional MNS should especially confuse motor imagery and motor observation, with the most discriminating voxels concentrated outside ventral MNS regions.

Alternatively, if traditional mirror neuron regions are key to action representation information, with other areas being mainly activated by attention and other factors, the most informative voxels should be concentrated in traditional MNS regions. Finally, a distribution of informative voxels across both MNS and non-MNS regions would suggest that action

representations are encoded throughout the wider AON, rather than solely in the traditional MNS.

To address whether parieto-frontal areas of overlapping activity can distinguish between our own (e.g., imagined) and others' (observed) actions, we also use multivariate (MVPA) methods to examine whether such areas do in fact carry information about each condition despite indistinguishable activation when analyzed with traditional functional magnetic resonance imaging (fMRI) methods. Finally, we investigate the relative amount of information regarding execution, observation and imagery of reaching carried by premotor versus posterior parietal areas.

Our results show that the voxels that contain information about action execution, observation, and imagery are distributed over both ventral/inferior and dorsal/superior premotor and posterior parietal regions, rather than being concentrated in isolated brain areas. This result challenges the supposed distinction between mirror neuron and nonmirror-neuron action observation areas. Unlike previous univariate analyses that could not differentiate between group-averaged activations for motor imagery and motor observation in premotor cortex and PPC (Filimon et al. 2007), MVPA successfully decodes imagined and observed reaching in areas activated equally strongly by these conditions, and successfully discriminates both from actual execution. This suggests that the brain could determine whether an action is observed, executed, or imagined, not merely based on primary sensory or motor areas, but also based on a finer-grained representation of information within jointly activated areas in the AON. Finally, we show that posterior parietal and premotor areas carry similar amounts of information regarding the observation, imagery, and execution of reaching. This suggests that both posterior parietal and premotor cortex play an integral role in motor representations, and could potentially be decoded equally well with neural prostheses.

Materials and Methods

We used MVPA (Norman et al. 2006) to analyze the fMRI data from Filimon et al. (2007), where univariate fMRI analyses revealed large overlapping activations for observation, execution, and imagery of reaching. Complete details of the behavioral task and fMRI data collection are provided in Filimon et al. (2007). In brief, 16 subjects performed 3 action-related tasks while undergoing functional magnetic resonance scanning in a 3T Varian scanner: actual reaching (Reach), observing a video clip of a hand reaching (Observe), and imagining oneself reaching (Imagine). All actions were toward images of abstract objects shown on a screen. Passive object viewing served as a baseline. Data from 2 participants were excluded because of excessive head motion and data reconstruction problems. Each participant completed at least two 8 min 32 s fMRI runs. Within each run, the 3 conditions plus baseline were each repeated 4 times, for 16 pseudo-randomized blocks of 32 s each. Within each block, there were eight 4-s trials. At the beginning of each block a visual message, for example, "reach", informed the participant of the upcoming task. The order of presentation for the baseline and 3 experimental conditions (observation, execution, and imagery) was pseudorandomly counterbalanced. Functional images were collected using an echo-planar T_2*-weighted gradient echo pulse sequence (3.75 × 3.75 × 3.8 mm voxel size, 28 contiguous axial slices, 64 × 64 matrix, time repetition (TR) = 2000 ms, 256 repetitions per scan, time echo (TE) = 27.4 ms, flip angle = 90°, bandwidth = 1950 Hz/pixel). After collection, the data were corrected for motion artifacts, registered to the anatomical images, and detrended in AFNI (Cox 1996).

Each participant's fMRI data were imported into Matlab for MVPA analysis using the Princeton Multi-Voxel Pattern Analysis Toolbox (www.pni.princeton.edu/mvpa). The time course of the blood oxygen level-dependent (BOLD) signal for each voxel was z-scored for each participant. Because of hemodynamic lag, the BOLD signal is delayed relative to the experimental time course. To limit carry-over of the BOLD signal between conditions due to the blocked design, the first and last 2 TRs were eliminated from each block. We used a region of interest (ROI) approach to select voxels for MVPA classification. Note that all ROIs were defined only in the left hemisphere because all (executed, observed, and imagined) movements were performed with the right hand, and Observe and Imagine led to much weaker or nonsignificant activations in the right hemisphere (see Filimon et al. 2007, Fig. 2). Classification between Reach, Observe, and Imagine based on strong Reach activations versus much weaker or nonsignificant Observe and Imagine activations in the right hemisphere would thus have been trivial, hence the focus on the left hemisphere only.

Two types of cortical ROIs were used for classification: functional overlap ROIs and anatomical ROIs. Functional overlap ROIs were identified as the regions of cortex that were significantly more activated than the passive viewing condition for all 3 experimental conditions using traditional general linear model (GLM) analysis (conjunction between Reach, Observe, and Imagine activations thresholded at $P < 0.001$ for each condition individually, uncorrected). The 3 conditions overlapped in PMd and intraparietal/superior parietal cortex (Filimon et al. 2007). This resulted in the selection of 2 separate functional overlap ROIs for each subject, one in dorsal premotor (PMd) cortex and one in PPC. Thus, in contrast to anatomical ROIs, which consisted of both ventral and dorsal premotor and parietal areas, the functional overlap ROIs were found only within PMd and intraparietal/superior parietal cortex, but not in Broca's area or IPL. Anatomical cortical surface ROIs were selected in individual subjects based on the Destrieux cortical surface atlas (Destrieux et al. 2010). Two anatomical ROIs were defined for each participant, one including all of left premotor (ventral, including Broca's area, and dorsal) cortex and the other including all of left posterior parietal (inferior and superior) cortex. Premotor anatomical ROIs included: the precentral sulcus, opercular and triangular parts of the IFG, the posterior part of the inferior frontal sulcus, middle frontal gyrus (MFG), superior frontal sulcus, as well as the vertical ramus of the anterior segment of the lateral sulcus. Posterior parietal anatomical ROIs included: the postcentral sulcus, supramarginal gyrus, angular gyrus, Jensen's sulcus, IPS, SPL, parieto-occipital sulcus (POS), the superior aspect of the precuneus, and the posterior end of the cingulate sulcus. These regions have previously been associated with reaching (Culham et al. 2006; Culham and Valyear 2006; Filimon et al. 2009, 2010; Gallivan et al. 2009; 2011; Cavina-Pratesi et al. 2010). These ROIs were defined on each subject's inflated cortical surface in Freesurfer (Dale et al. 1999; Fischl et al. 1999) and converted to volume masks. We refer to these as the anatomical premotor and PPC ROIs. Care was taken to avoid primary somatosensory (S1) and motor (M1) areas as well as the entire occipital lobe, as we were interested in areas activated by all 3 conditions, rather than areas activated predominantly or only by motor execution or visual stimulation. Although subthreshold activation in these areas by nonpreferred conditions cannot be ruled out, classification between the 3 conditions based on M1 or the occipital lobe would have been trivially easy because of significantly weaker activation in one condition compared with the others. For both functional overlap and anatomical ROIs, all analyses were done using the premotor and PPC areas both individually and in combination. The average number of voxels per ROI is given in Table 1.

While the main focus of this paper is on parieto-frontal circuits, we also ran an additional MVPA analysis on occipito-temporal (OT) voxels, given recent reports of an OT involvement in both visual and motor execution aspects of movement and body part representations (Astafiev et al. 2004; Bracci et al. 2010; Oosterhof et al. 2010; Orlov et al. 2010; Valyear and Culham 2010). Due to very weak Imagine activations in OT cortex in our univariate fMRI analysis (Filimon et al. 2007), we defined OT ROIs by computing a conjunction between Reach (vs. baseline, i.e., passive observation of objects) and Observe (vs. baseline) within each individual subject, using a threshold of at least $P < 0.05$ for each condition.

Table 1
Mean ROI sizes in voxels

	Premotor	Parietal	Combined
Anatomical			
Full ROI	695 (116)	1,408 (220)	2,102 (299)
Most important 10%	70 (11)	141 (22)	211 (30)
Least important 90%	624 (104)	1,266 (198)	1,891 (269)
Overlap			
Full ROI	98 (49)	182 (104)	281 (144)
Most important 20%	20 (10)	37 (21)	57 (29)
Least important 80%	78 (39)	145 (83)	224 (115)

SDs are given in parentheses.

For all ROIs, we first directly assessed the discriminability of patterns of activation in the experimental conditions. Support vector machines (SVMs) were trained in binary classification between pairs of the conditions (Observe vs. Imagine, Reach vs. Imagine, and Observe vs. Reach). The SVMs were trained and evaluated using MEX-SVM (Briggs, http://tinyurl.com/b2uy3v5), an interface to SVM-light (Joachims 1999). Linear kernels were used throughout. Nonlinear kernels were tested, but did not improve generalization accuracy. Linear SVMs combine the activations across several variables according to learned weights to make a decision about category membership. Cross-validation was used to form independent training and holdout generalization sets to obtain an unbiased estimate of classifier performance. Classification performance was evaluated separately for each participant using either 4- or 6-fold cross-validation (4 for participants completing 2 functional runs, and 6 for participants completing 3 runs). Cross-validation is a method to assess the accuracy of classification on untrained data by iteratively holding out a subset of data, training the classifier on the remaining data, and testing accuracy on the holdout set. For example, to classify between the Reach and Observe conditions for a participant completing 2 runs, all TRs from the Reach and Observe conditions were selected. One quarter of the data were withheld as a holdout set to test generalization accuracy. The withheld data consisted of complete and adjacent blocks within a session. The classifier was trained using the remaining data. Finally, the trained classifier was used to predict the conditions for the withheld dataset. This process was repeated, holding out each quarter of the remaining data for testing. Accuracy was averaged across these cross-validation runs to determine the average accuracy of the classifier. All presented accuracy results are for generalization holdout sets.

Using the trained classification weights, the importance of each voxel was determined in an identical manner to the analysis used by Hanson and Halchenko (2008). A linear SVM is simply a linear classifier, that is, a particular vector of voxel values $\mathbf{x} = (x_1, x_2, \ldots, x_n)$ (where n is the number of voxels) is classified based on a learned weight vector $\mathbf{w} = (w_1, w_2, \ldots, w_n)$ and bias b, depending on whether $\mathbf{w} \cdot \mathbf{x} + b = \sum_i w_i x_i + b$ is greater or less than 0. The importance of each voxel i is defined as the square of the corresponding coefficient w_i, that is, the voxels with the smallest w_i^2, and hence, the smallest contribution to the decision, are the least important.

Given the large number of voxels used in classification, especially for the anatomical ROIs, we additionally applied recursive feature elimination (RFE) (Guyon et al. 2002) to find the most important voxels. RFE iteratively removes the least important voxels as measured by w^2 while tracking classification error. Determining the expected final accuracy for any particular set of voxels based on observed accuracy during RFE requires an extra holdout set to ensure a lack of bias in final accuracy estimates. In essence, 2 nested cross-validations must be performed. The procedure is as follows: starting from each full ROI, the 2 voxels with the smallest w^2 are eliminated and the classifier is retrained with the remaining data. At each elimination step, generalization performance is tested on the inner holdout set. Performance on the inner holdout set is used to determine when the classifier accuracy has deteriorated compared with using the full set of voxels. Performance on the outer holdout set is used as a final assessment of accuracy. This procedure was conducted separately for each participant, comparison, and starting ROI. Note that this is a greedy search procedure, and therefore is not guaranteed to find an optimal set of voxels for classification. After observation of generalization accuracy during elimination, cutoff points were identified as the longest surviving 10% of the original voxels in the case of anatomical ROIs, and 20% for the overlap ROIs (which start with fewer voxels). These proportions were selected from the results of generalization accuracy on the inner holdout set as voxels were removed, representing the smallest proportion of voxels needed to achieve a high level of performance (see Fig. 2). Accuracy with the outermost validation holdout was measured using the most influential voxels alone (how accurate is the classifier with the best alone), only the eliminated voxels (how accurate is the classifier without the best), and finally the lowest 50% of all voxels (how accurate is the classifier using only the least influential 50% of voxels). Note this entire RFE procedure is repeated for each validation holdout set separately, keeping the analyses entirely independent.

Visualization and Localization

To visualize the contribution of each voxel's activation toward either Reach, Observe, or Imagine, we trained SVMs to discriminate each condition from the other 2 using the combined premotor and parietal anatomical ROIs. This was done in a manner otherwise identical to that used for the direct 2-condition comparisons. We plot the weights from these comparisons and ROIs to enable straightforward interpretation in a compact format. Each voxel's importance (defined as w_i^2—see Materials and Methods) was averaged over cross-validation runs, mapped to each subject's cortical surface, and then averaged over subjects.

Weights resulting from training one condition versus the others were used for visualization to facilitate interpretation of the weights in the context of a single condition. As a check that weights learned through training to discriminate a condition from both others were analogous to weights learned from direct 2-condition comparison, we compared weights learned from both methods. The learned weights for classification of one condition versus the other 2 corresponded closely to the weights learned using 2-condition discrimination (e.g., weights for Observe vs. Reach are very similar to the weights for Reach versus Others subtracted from the weights from Observe versus Others, mean correlation = 0.93, standard deviation [SD] = 0.044). Additionally, importance values learned in corresponding areas of the combined premotor and parietal ROIs (presented in Fig. 3) were very similar to those learned considering either premotor or parietal ROIs independently; the mean correlation between values learned in the combined parietal and premotor ROI and the individual ROIs was 0.95 (SD = 0.040).

Although MVPA identifies distributed voxels without regard for how such voxels cluster, to provide anatomical (MNI) x, y, z coordinates of voxels important for MVPA classification, we also performed a cluster analysis on the learned MVPA weights. We used a growing threshold method (Hagler et al. 2006) where we checked for clusters at different cluster sizes and P values. Clusters over 50 mm^2 over a threshold corresponding to $P = 0.05$, 40 mm^2 at $P = 0.01$, 20 mm^2 at $P = 0.005$, or 15 mm^2 at 0.001 were identified, and MNI x, y, z coordinates of the center of these clusters were recorded.

Results

Discrimination of Executed, Observed and Imagined Reaching

Figure 1 shows the generalization accuracy for every comparison and ROI, averaged over cross-validation folds. Accuracy was significantly above chance for all comparisons and ROIs (all $t_{13} \geq 5.34$, $P \leq 0.002$, Holm 1979 corrected). Chance performance for the comparisons is 50% correct.

It is not surprising that the classifier was able to discriminate between Reach and the other conditions, as actual reaching typically shows greater activity, even in areas of overlapping activation. However, unlike traditional GLM analyses, MVPA was able to discriminate between observation and imagery of reaching at above chance levels using the BOLD activation across multiple distributed and commonly activated voxels.

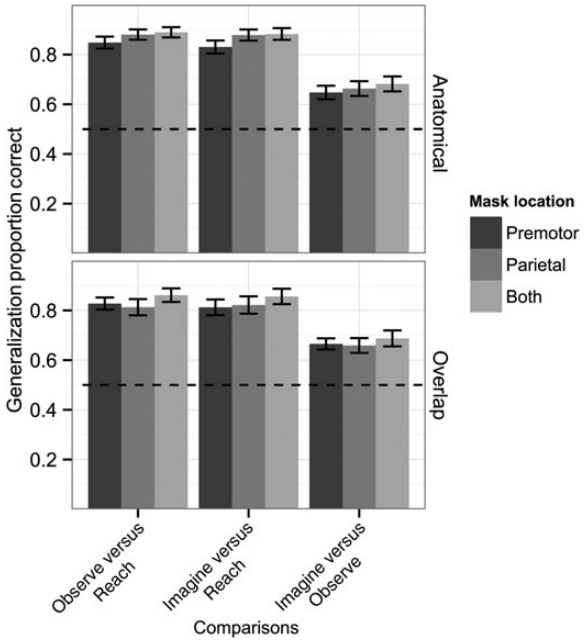

Figure 1. Generalization accuracy for each classification, ROI (mask) type and ROI location. Parietal and premotor regions of functional overlap (Overlap ROIs) were selected based on the overlap between Reach, Observe, and Imagine activations versus baseline (each at $P < 0.001$, uncorrected), using traditional GLM analysis. These functional overlaps resulted in the selection of a left dorsal premotor (PMd) and a left posterior parietal cortical (PPC) area (see Materials and Methods). These overlap ROIs included dorsal premotor and intraparietal/superior parietal cortex, but not ventral premotor/Broca's area or IPL, since there was no functional overlap in ventral areas. The anatomical ROIs were selected based on the Destrieux cortical surface atlas, and consisted of (1) all of left premotor (ventral and dorsal, as well as Broca's area) and (2) all of left posterior parietal (inferior, intraparietal, and superior) cortex (see Materials and Methods). As indicated, classifiers were trained using either the individual premotor or parietal ROIs, or the combination of both. The dashed lines indicate chance performance of 50%. Error bars are ±1 standard error of the mean over subjects, after averaging over cross validation runs.

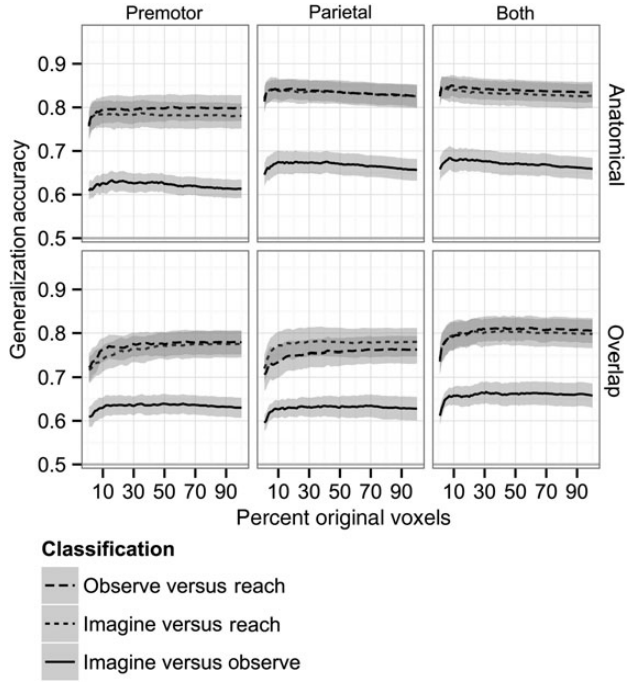

Figure 2. Results of the voxel elimination analysis. Generalization accuracy for the full ROI is the right-most point on each curve; moving toward the left more and more voxels are eliminated. Table 1 provides statistics on the number of voxels in each ROI. Because each participant started with a different size ROI, feature elimination contained unique numbers of voxels at each step for different subjects. Thus, to plot across-participant averages, generalization accuracies were linearly interpolated to a common set of points for all participants. The shaded region corresponds to ±1 standard error of the mean averaged over participants, after averaging cross-validation runs for each individual participant. Chance performance is 50%.

Although Observe and Imagine activations were discriminable with MVPA, they were more similar to each other than to Reach (Observe vs. Reach compared with Observe versus Imagine, $t_{83} = 17.11$, $P < 0.001$; Imagine versus Reach compared with Imagine versus Observe, $t_{83} = 15.85$, $P < 0.001$).

Despite the fact that the overlap ROIs were ~13% the size of anatomical ROIs (see Table 1), classification in the overlap ROIs was still above chance, and only 2.2 percentage points lower than accuracy using anatomical ROIs, on average. Furthermore, in the overlap ROIs, by definition, the conditions were all highly significant ($P < 0.001$, uncorrected) versus baseline. Unlike the anatomical ROIs, which included Broca's area and the IPL, overlap ROIs consisted of only PMd and intraparietal and superior parietal cortices. Thus the conditions could be discriminated based on both superior (dorsal) ROIs (which excluded PMv/Broca's and the IPL), and based on ROIs that included PMv/Broca's and the IPL (see also below for visualization of ventral vs. dorsal distributions of discriminating voxels). The discriminability using the overlap ROIs suggests a finer-grained pattern of voxel activation across conditions, even in robustly and commonly activated voxels within areas of functional overlap.

Relatively Small Numbers of Voxels Contain Sufficient Information for Discrimination

A second test was conducted to examine the distribution of discriminative voxels in each of the anatomical and overlap ROIs. This analysis recursively eliminated voxels with small classifier weights to assess whether small, but informative, subsets of voxels could reliably discriminate between conditions. Figure 2 presents generalization accuracy for comparisons between conditions as voxels are eliminated from each ROI. Accuracy remained high even with a much smaller number of voxels; remaining relatively stable until ~90% of the voxels were eliminated from the anatomical ROIs, after which performance rapidly dropped to chance. Note that with anatomical ROIs, which started with over 5 times the number of voxels compared with the overlap ROIs on average, generalization accuracy improves slightly with feature reduction. This suggests that cutting out irrelevant voxels reduced noise, increasing accuracy. Additionally, for many of the comparisons, particularly Reach versus the other conditions, accuracy of just the last 2–3 voxels surviving elimination (the far left of each curve in Fig. 2, i.e., the lowest percentage of original voxels) was quite high. This is especially interesting given that these accuracies are based on generalization to unseen data, using cross-validation; that is, they are not based on peculiarities of the training data. Figure 2 also reveals that the difference in accuracy for classification between Imagine and Observe remains relatively constant as voxels are eliminated. The overlap ROIs, containing fewer voxels at the start, were more affected by voxel elimination, with accuracy degrading after elimination of ~80% of the original ROI voxels.

After the elimination process was complete, we tested accuracy on an independent final validation set using the most informative voxels, defined as the cutoff with approximately maximum

accuracy for the elimination procedure: the top 10% for anatomical ROIs, and the top 20% for overlap ROIs. Figure 3 shows generalization accuracy on the final holdout set using the most important voxels. Accuracies were significantly above chance for every comparison and initial ROI type (all $t_{13} >= 5.48$, $P < 0.001$; all Holm corrected).

Information Still Exists in the Eliminated Voxels

While a small number of voxels is sufficient to discriminate between conditions, we also found that the conditions could be discriminated using only the *eliminated* voxels in both anatomical and overlap ROIs, indicating that condition information is also spread throughout the ROIs and is not isolated within a few voxels. In the least informative 90% or 80% of voxels, for anatomical and overlap ROIs respectively, accuracy was still high and significantly above chance for all comparisons (all $t_{13} \geq 5.06$, $P < 0.001$, Holm corrected). It was lower than using the most important voxels by only 3.2 percentage points on average. We additionally tested classification accuracy using only the first 50% of voxels eliminated for each comparison (lowest 50%), and found that this accuracy was also above chance for all comparisons (all $t_{13} \geq 3.20$, $P \leq 0.005$, Holm corrected), suggesting that successful classification is not due simply to voxels just below our threshold for importance (i.e., the 11th–20th percentile is not driving accurate performance). These findings indicate that BOLD activations for observed, imagined, and actual reaching are discriminable not only using the pattern of activation in a small subset of voxels,

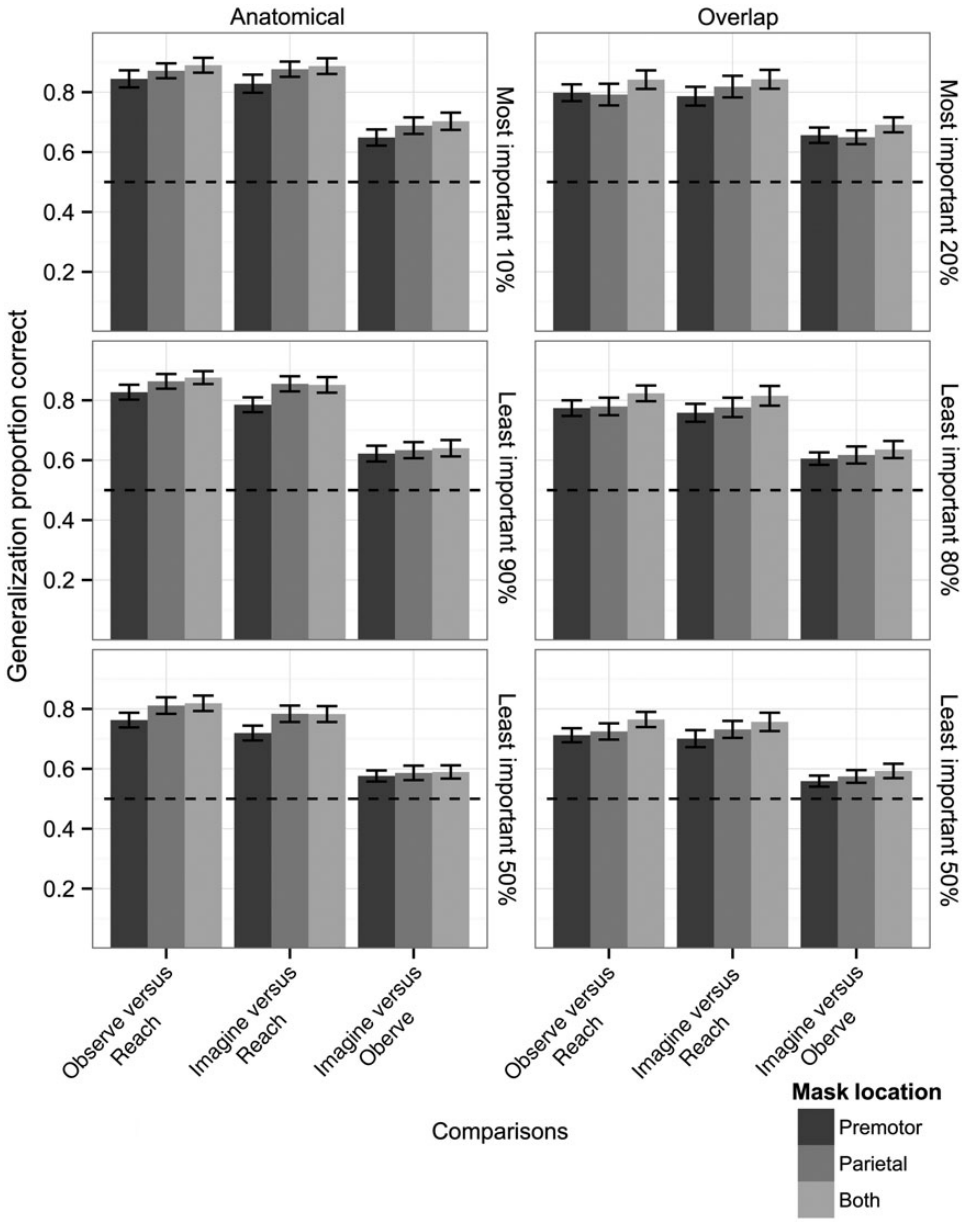

Figure 3. Accuracy on the final independent test set in each of the conditions for each of the ROIs (masks). For the anatomical ROIs these classifications used the final, most important, 10% of voxels or the least important 90% of voxels which were first eliminated. For the overlap ROIs, accuracy was assessed for the top 20% of voxels and for the 80% first eliminated. Both types of ROIs were also evaluated using the first eliminated, and thus least important, 50% of voxels. Chance performance was 50% and is indicated by the dashed lines. Error bars are ± 1 standard error of the mean over subjects, after averaging over cross validation runs.

but also based on pattern differences among a much wider set of voxels. These results are consistent with pattern classification of single unit activity in macaques, where as few as 16 neurons suffice for accurate decoding of a particular grip type from area F5 (Carpaneto et al. 2011). The fact that information is both concentrated in small numbers of strongly predictive neurons, and distributed across many, more weakly predictive neurons, suggests robustness to injury via redundancy.

The accuracy in overlap ROIs suggests that our own or others' actions, as well as our imagined actions, are distinct within commonly activated premotor and parietal areas independent of differences in M1 or primary sensory (visual, tactile) activations. Thus, although voxels that are part of the AON are co-activated for observation, imagery, and execution of action, subtle differences in the activation patterns among subsets of such networks are able to distinguish between these conditions. The success of classification using the least important weights argues for widely distributed discriminative information about Reach, Observe and Imagine.

Note that even if it were to be assumed that the Reach condition is trivially easy to discriminate from the other 2 conditions, due to globally greater levels of activation, this could not account for above-chance classification between Imagine and Observe, which had equal overall levels of activation (see Filimon et al. 2007). Even within the most and least important voxel subsets of the overlap ROIs, Imagine and Observe continue to be discriminable with accuracy between 60% and 71% (with chance at 50%).

Discriminating Voxels are Distributed Over Both Dorsal and Ventral Areas

Figure 4 presents the learned weights from training to discriminate each condition from the other 2 in the combined anatomical ROIs, averaged over all participants and cross-validation runs. The location of commonly activated areas for Reach, Observe, and Imagine in premotor cortex and PPC, corresponding to the overlap ROIs (see Materials and Methods), is shown using a black outline. Figure 5 displays the 10% of weights with the highest magnitude for 4 individual subjects. The magnitude of the weight corresponds to the contribution of that voxel to the separability of the 2 conditions (Hanson and Halchenko 2008). Each voxel has a learned weight for each of the 3 comparisons, Reach versus Other, Observe versus Other, and Imagine versus Other. The sign of each weight corresponds to which condition the activation in that voxel provides evidence for. Positive weights (red to yellow) give evidence for the condition of interest (e.g., for Reach in Reach vs. Other), and negative weights (blue to light-blue) are evidence for the Other conditions. Thus the colors represent the weight of evidence for or against a particular condition, not activation magnitude (relative to baseline) as in traditional univariate BOLD signal figures. A higher magnitude weight provides more evidence for the appropriate condition when that voxel is active. The magnitude of the weight is illustrated by the brightness of the color.

Figure 4 shows that the weights discriminating between different conditions were spatially distributed across both dorsal (superior) and ventral (inferior) areas in both premotor and posterior parietal cortices, across all subjects. Importantly, weights provided evidence both for and against a condition even within the overlap ROIs, that is, even within areas commonly activated by all 3 conditions above baseline (see red and blue weights within the black outlines, Fig. 4). This suggests condition-specific fine-grained patterns of activation even within areas significantly and positively activated by each condition.

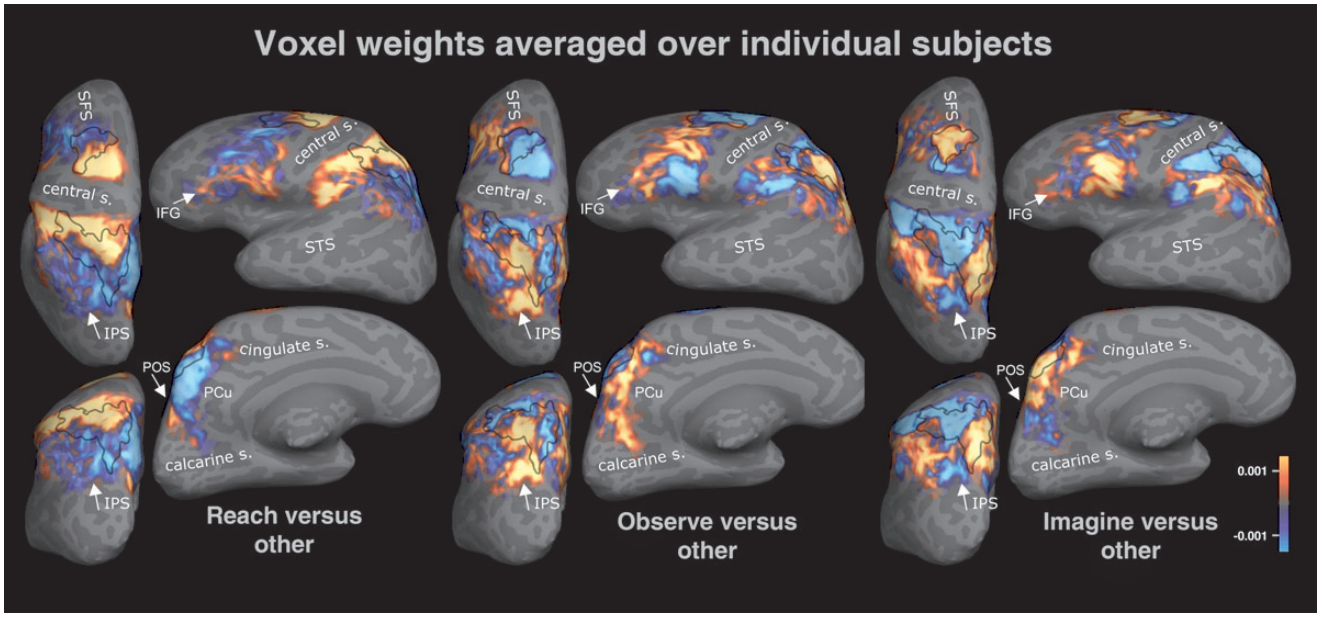

Figure 4. Visualization of each voxel's learned weights for classification of one condition versus both others. The learned anatomical ROI weights for each comparison and each voxel averaged over the 14 subjects are plotted on the cortical surface for the 3 classifiers. The corresponding overlap ROIs are also outlined in black. Red-to-yellow indicates a positive weight for the corresponding voxel, that is, where activation indicated evidence for the indicated condition. Blue-to-light-blue indicates a negative weight, and thus activation of the corresponding voxel is evidence against that condition. The magnitude of the weight is indicated by the brightness of the color (see color bar). The color bar ticks indicate weight values of ± 0.001. Note that since the task involved execution, observation, or imagery of the right hand, only the left hemisphere was included in the ROIs, and therefore plotted here. Abbreviations: IPS, intraparietal sulcus; SFS, superior frontal sulcus; IFG, inferior frontal gyrus; STS, superior temporal sulcus; s., sulcus; POS, parieto-occipital sulcus; PCu, precuneus. Putative human PMd is located at the posterior end of the SFS. Putative human PMv is located anterior to the inferior aspect of the central sulcus, toward the posterior end of the IFG.

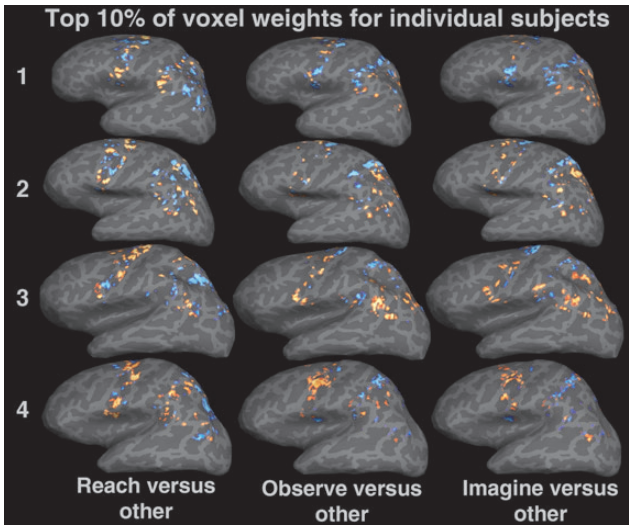

Figure 5. Visualization of learned weights for the most important 10% of voxels from 4 participants. These are the top 10% of voxels that were most important to classification using the anatomical ROIs as estimated by the elimination procedure. Weights for these individual subjects are plotted in an analogous manner to Figure 4.

The individual activations in Figure 5 show that even the 10% of voxels with the largest magnitude weights are distributed across both dorsal and ventral areas. The exact pattern of spatial distribution of the top 10% of voxel weights was idiosyncratic, however. For example, although top 10% weights were distributed across dorsal, middle, and inferior frontal cortex, subjects exhibited unique patterns of weights providing evidence for and against a condition (e.g., in Fig. 5, Subject 1 showed both red and blue (positive and negative) weights for Observed Reaching in PMv, whereas Subject 3 showed mostly red (positive) weights for Observed Reaching in PMv). The unique pattern of activations and weights highlights the importance of single-subject analysis in addition to group averages, where group-averaged activations might wash out due to differences between subjects.

Information is Contained in Both Premotor and Parietal Areas

Notably, classifier accuracy was similar using either the individual premotor or parietal ROIs (both anatomical and overlap), suggesting that representations of imagined, observed, and executed reaching are similarly distinct in the premotor and posterior parietal areas examined. There were no significant differences between classification accuracy in premotor and parietal ROIs for any of the comparisons (Fig. 1; all $|t_{52}| \leq 0.98$, $P \geq 0.33$, n.s.; without multiple-comparison correction). For both anatomical and overlap ROIs, accuracy using the combined parietal and premotor ROIs was slightly higher compared with individual ROIs (Fig. 1, between pairs of conditions, both−parietal, $t_{83} = 7.14$, $P < 0.001$, both−premotor, $t_{83} = 6.00$, $P < 0.001$).

Topographical Organization of Execution, Observation, and Imagery of Reaching

Despite the wide distribution of the most informative voxels for each condition (Fig. 5), Figure 4 nonetheless shows that the voxel weights were distributed in different topographical patterns for each condition across the cortical surface.

In the frontal lobe, higher activation of PMd (posterior part of the superior frontal sulcus) provided stronger evidence for Reach (see red-yellow weights) rather than other conditions. Activation of anterior parts of PMd showed evidence for Imagine. Within the overlap ROI in PMd, the most posterior activations provided evidence for Reach but against Imagine, with mixed evidence for Observe. Anterior activations provided evidence against Reach and for Imagine (Fig. 4). This suggests a topographical organization of PMd, with posterior parts providing evidence for actual reaching and anterior parts providing evidence for imagined reaching. Despite also activating PMd significantly above baseline ($P < 0.001$, see Materials and Methods), activations within the overlap ROI mostly provided evidence against Observe, except for a small activation lateral and posterior in the PMd overlap ROI. Thus, in contrast to traditional fMRI analyses, where Imagine and Observe did not appear to differ in their activation of PMd (Filimon et al. 2007), MVPA reveals different patterns of weights within PMd, with the same voxels providing different evidence for or against Imagine and Observe. Superior frontal voxels did provide evidence for Observe compared with Reach and Imagine, but were generally located anterior to the overlap ROI in PMd.

More laterally, activations in the MFG provided evidence for Observe but against Reach, and mixed evidence for and against Imagine. In IFG and PMv posterior voxels provided evidence for Reach and Imagine, but against Observe, whereas anterior voxels generally provided weak evidence for or even against Reach and Imagine, but strong evidence for Observe.

Thus, in general, across the frontal lobe evidence for Reach was more similar to Imagine than to Observe, consistent with both reaching and imagined reaching involving self-action, as opposed to the actions of another agent. Evidence for Reach was generally more posterior (closer to the central sulcus) in both dorsal and ventral premotor areas.

Although frontal lobe motor-related activation weights showed a distributed spatial pattern (from dorsal to ventral premotor regions), and similar patterns for Imagine and Reach, there were also unique patterns of interwoven evidence for and against each condition. Thus instead of a homogeneous, unitary representation, this finer-grained representation of information even in Broca's area (IFG) and in PMv shows that activation is mixed both for and against Observation in these regions.

The posterior parietal lobe similarly showed interleaved patterns of evidence both for and against each condition. Broadly, higher postcentral sulcus activation was strong evidence for Reach and against Imagine (dorsal and lateral views, Fig. 4). Postcentral sulcus (post-CS) weights were mixed both for (lateral post-CS) and against (middle post-CS) Observe. Thus, whereas in the frontal lobe Reach and Imagine weights were similar, in PPC, Reach and Imagine showed almost exactly opposite patterns of weights, with voxels that provided evidence for Reach providing evidence against Imagine. Observe showed a mixed pattern of weights, but generally reversed compared with Imagine.

In the IPL, activation of the supramarginal gyrus (SMG, lateral view, extending into putative human AIP) presented positive evidence for Reach but mixed (and generally opposite) evidence for Observe and Imagine. Angular gyrus voxels showed mixed and opposite patterns for Observe and Imagine, with stronger evidence for Imagine, and mostly evidence against Reach.

Posterior IPS provided evidence against Reach and Imagine but for Observe (Fig. 4). Medial parietal cortex (precuneus, PCu) activations provided similar support for Observe and Imagine, but against Reach, with the exception of the posterior

end of the cingulate sulcus and most superior/anterior aspect of the precuneus (a possible homolog of macaque PEc), which provided evidence for Reach and against Imagine and Observe (medial view). This positive evidence for Reach in anterior/superior PCu was an extension of weights providing positive evidence for Reach in medial IPS and the anterior part of the superior parietal gyrus (putative MIP; Filimon et al. 2009). Putative MIP showed negative or mixed evidence for Observe and Imagine. At the POS in posterior PCu, a small area just posterior to the POS, putative V6 (Pitzalis et al. 2013) indicated positive evidence for Reach, negative evidence for Imagine, and mixed or weak evidence for Observe. Just anterior to the POS (sPOS, or putative V6A; Filimon et al. 2009), the pattern for Imagine and Reach reversed, with negative weights for Reach and positive evidence for Imagine. Note, however, that the putative human homologs of macaque parietal areas are not fully established and remain to be delineated (see, e.g., Filimon et al. 2013, for putative human LIP).

As in premotor cortex, the posterior parietal overlap ROI, which included the IPS and superior parietal gyrus, also showed mixed evidence for and against each condition, despite common and significant above-baseline ($P < 0.001$) activation across all 3 conditions in the overlap ROI. In contrast to premotor cortex, Reach and Imagine showed opposing patterns in the posterior parietal overlap ROI, with Reach and Observe being more similar to each other in the parietal overlap ROI.

Overall, as in the frontal lobe, posterior parietal weights exhibited a (reversed) posterior-to-anterior gradient, with more anterior voxels providing stronger evidence for Reach than for Observe and Imagine, and more posterior voxels providing evidence against Reach but mixed evidence for Observe and Imagine. The mixture of evidence for and against each individual condition additionally suggests that despite common activation, distributed voxels show unique patterns of activation that uniquely predict each condition. Tables 2–4 provide the results of the cluster analysis, showing distributed regions important for classification across the ROIs.

Figure 6 presents the MVPA results within OT cortex. Accuracy was high and well above chance for all comparisons. Note that Imagine was highly discriminable from the other conditions within OT primarily due to a general lack of activation in OT during motor imagery (see predominantly blue weights for Imagine vs. Other in OT in Fig. 6), consistent with our previous results (Filimon et al. 2007). However, a certain topography can be observed within OT: posterior voxels within the OT ROI show negative weights for (evidence against) Imagine but positive weights for (evidence for) Observe. More anterior and superior OT weights were positive for Imagine but negative for Observe, whereas Reach weights were positive across both anterior and posterior OT. This is consistent with Observe leading to more posterior, visual activation in OT, and with motor imagery and execution relying on more "motor" regions in anterior OT. Reach, unlike Imagine, also led to visual stimulation, consistent with the anterior–posterior extent of positive weights for Reach in OT. The distinct topography between imagery, observation, and execution suggests that different parts of OT may play different roles in action representation.

Discussion

Our findings shed light on 3 key questions that have emerged from the literature on the neural substrates of action

Table 2
Executed Reaching versus Imagined and Observed Reaching

Brain region	Area (mm^2)	max. t	MNI coordinates (center voxel)		
			x	y	z
Dorsal central sulcus (PMd/M 1)	20.05	6.04	−25.0	−23.4	59.5
Superior parietal gyrus/precuneus	25.04	−5.50	−7.5	−66.9	51.8
Medial IPS	27.32	7.92	−28.7	−55.1	53.5
Anterior IPS	34.58	8.19	−33.9	−46.8	35.4
Superior POS	38.15	−3.39	−15.3	−77.1	43.0
Dorsal precentral gyrus (PMd)	48.97	10.08	−34.7	−23.4	49.9
Inferior precentral sulcus (PMv)	53.06	−2.17	−43.4	6.4	19.1
IPS	53.07	7.79	−32.2	−49.7	48.6
Inferior precentral gyrus	53.48	−3.02	−51.9	−4.5	41.4
Superior occipital gyrus/sulcus	65.72	−3.01	−25.1	−74.9	23.4
Superior occipital sulcus	67.24	−3.39	−32.5	−75.2	23.7
Posterior Sylvian fissure	68.97	7.93	−42.3	−38.2	19.2
Middle occipital gyrus	73.32	−2.16	−40.3	−78.7	13.4
Supramarginal gyrus	74.83	6.19	−52.0	−43.5	42.6

Clusters of voxels whose weights discriminate between Executed Reaching versus Imagined and Observed Reaching in MVPA classification. Above baseline activation in areas with positive maximum t values indicates evidence for the Reach condition, while above baseline activation in areas with negative maximum t values indicates evidence against the Reach condition. PMd, dorsal premotor cortex; PMv, ventral premotor cortex; M1, primary motor cortex; IPS, intraparietal sulcus; POS, parieto-occipital sulcus.

Table 3
Observed Reaching versus Executed and Imagined Reaching

Brain region	Area (mm^2)	max. t	MNI coordinates (center voxel)		
			x	y	z
Middle occipital gyrus	24.66	6.42	−35.5	−82.6	20.4
Posterior IPS	29.07	6.90	−28.3	−65.3	37.4
ventral precentral gyrus (PMv)	46.11	−3.01	−52.4	3.8	3.2
Dorsal central sulcus (PMd/M1)	46.60	−4.20	−29.9	−24.5	52.6
Precentral gyrus (PMd)	52.42	−4.20	−36.6	−20.6	55.4
Middle insula	55.81	−2.16	−42.9	−0.3	13.5
STG/posterior Sylvian fissure	69.48	−3.01	−56.6	−42.1	16.1
precuneus	77.89	4.12	−8.7	−63.4	50.5
Medial IPS	83.37	−2.16	−34.1	−48.3	48.1
POS	158.10	4.51	−10.0	−63.5	23.7
Superior occipital gyrus	160.64	−2.17	−19.5	−68.1	42.5

Clusters of voxels whose weights discriminate between Observed Reaching versus Executed and Imagined Reaching in MVPA classification. Above baseline activation in areas with positive maximum t values indicates evidence for the Observed Reaching condition, while above baseline activation in areas with negative maximum t values indicates evidence against the Observed Reaching condition. STG, superior temporal gyrus; also see Table 1.

Table 4
Imagined Reaching versus Executed and Observed Reaching

Brain region	Area (mm^2)	max. t	MNI coordinates (center voxel)		
			x	y	z
Superior Parietal gyrus	27.10	7.00	−10.7	−69.5	53.6
Anterior IPS	29.43	−4.20	−33.6	−45.3	39.5
posterior Sylvian fissure/STG	33.93	5.06	−58.1	−46.1	18.4
Posterior STS	34.41	5.26	−40.1	−66.9	29.8
Supramarginal gyrus	43.22	−3.40	−53.0	−47.6	38.3
Superior occipital gyrus	47.02	6.86	−20.0	−73.6	37.9
Dorsal central sulcus (PMd/M1)	50.40	−2.16	−34.3	−23.8	46.2
Anterior insula	53.12	3.11	−36.1	14.5	11.9
Dorsal precentral sulcus (PMd)	58.68	3.70	−27.7	−13.0	54.5
Middle occipital gyrus	63.10	−2.16	−34.7	−83.4	17.4
Posterior Sylvian fissure	88.36	−2.16	−39.7	−37.3	16.3
Ventral precentral gyrus (PMv)	152.41	4.40	−51.4	4.3	4.8

Clusters of voxels whose weights discriminate between Imagined Reaching versus Executed and Observed Reaching in MVPA classification. Above baseline activation in areas with positive maximum t values indicates evidence for the Imagined Reaching condition, while above baseline activation in areas with negative maximum t values indicates evidence against the Imagined Reaching condition. STS, superior temporal sulcus; also see Table 1.

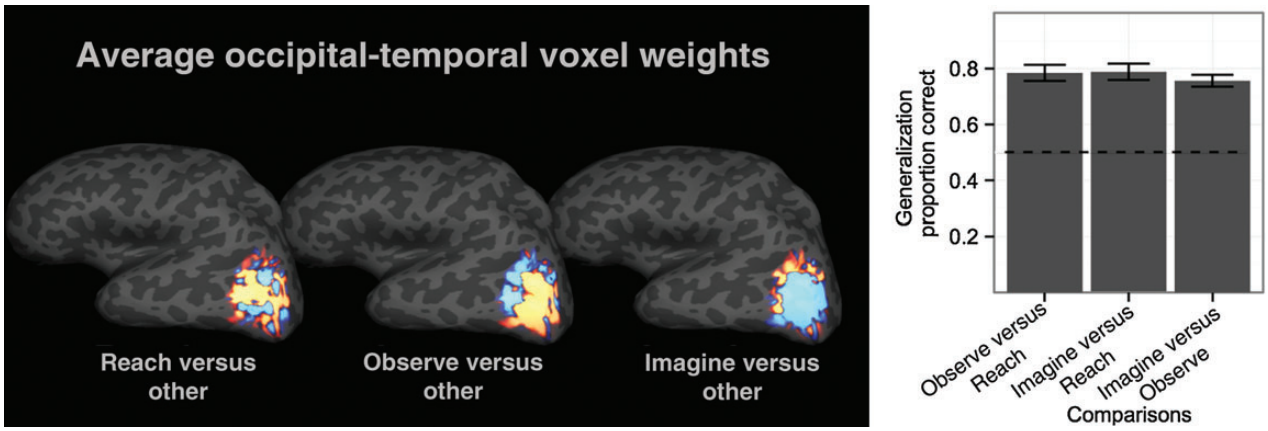

Figure 6. Left: visualization of learned weights using the OT mask plotted in a manner analogous to Figure 4. Right: MVPA accuracy using these masks for listed comparisons.

observation, execution, and mental imagery. We discuss these in detail below. First, our MVPA results provide evidence that action-related information, including action observation, is not just concentrated in a small number of brain regions analogous to the IPL-F5 mirror neuron circuit in the macaque, but is instead extensively distributed across multiple areas, both dorsal and ventral. Second, we used MVPA to show that the patterns of activation *within* commonly activated regions are distinct for observation, execution, and imagery. Third, we address the question of frontal versus parietal motor dominance, and show that both areas contain motor representations that are similarly discriminative between execution, observation, and imagery of hand movements.

Action-Related Information is Distributed Across Both Ventral and Dorsal Regions

Our results (see Figs 4 and 5) show that the voxels most discriminating between conditions are highly spatially distributed, not only in the anatomical ROIs, but even within the overlap ROIs defined by overlapping activations. Note that, unlike traditional univariate fMRI analysis, MVPA allowed us to identify which voxels are predictive of a particular condition, despite being activated by multiple conditions. Importantly, MVPA identified distributed informative voxels that significantly predicted each condition, rather than requiring voxels to be clustered and activated above a particular threshold as in univariate fMRI analyses. In our frontal lobe anatomical ROIs, the most discriminating voxels were located in the IFG, ventral premotor, dorsal premotor, and middle frontal cortices. This suggests that the most useful information for distinguishing between execution, observation, and imagery of reaching is not concentrated in one anatomical region (e.g., either within or outside areas activated by all 3 conditions), but is instead represented throughout premotor and other frontal areas. The same pattern of widely distributed information held in the PPC. Discriminative information was contained not only in the IPL, but also in voxels located in the IPS, superior parietal gyrus, and the precuneus. This was true for each condition, including observation. This suggests that Broca's area and the IPL, which are part of the traditional mirror neuron circuit, do not contain more or less discriminative activations indicating action observation than dorsal areas, and that instead even for observation, useful information is distributed across voxels located in multiple anatomical areas, both ventral and dorsal. This challenges the assumed dominance of traditional mirror neuron areas for representing observation of action, which would have predicted differential discriminability in traditional mirror neuron versus nonmirror-neuron areas. Moreover, the patchwork of discriminative voxels within and outside traditional mirror neuron areas calls into question whether all of Broca's area (or PMv) should be considered *a* mirror neuron *area*, that is, as if the entire area consisted of mirror neurons. Clearly, activations within PMv and Broca's area are heterogeneous. Both premotor cortex and PPC exhibited a posterior–anterior gradient in weights, with more posterior frontal weights and more anterior parietal weights providing stronger evidence for Reach than the other 2 conditions. This is consistent with previous reports of posterior–anterior gradients in visual versus motor preference, including macaque neurophysiological research on reach-related neuronal firing in multiple cortical areas (Johnson et al. 1996; Burnod et al. 1999; Battaglia-Mayer et al. 2001, 2003; Caminiti et al. 2010; Gamberini et al. 2011) and distributed fMRI activations for reaching (Medendorp et al. 2005; Filimon et al. 2009; Filimon 2010). The distributed pattern of weights and activations also challenges the idea of a single parietal reach region (see Filimon et al. 2009). In addition, the fact that reaching can be decoded from both superior and inferior parietal regions is consistent with recent evidence that the reach and grasp pathways are intermingled (Fattori et al. 2009; Fattori et al. 2010; Monaco et al. 2011). The lack of a strict segregation between reach and grasp pathways has also been documented in frontal regions: reaching is also represented in PMv (Gentilucci et al. 1988; Gregoriou and Savaki 2003; Gregoriou et al. 2005), while PMd also represents grasping (Raos et al. 2003; 2004b). This suggests that such wide distribution of informative voxels may also hold for observation of grasping, not just reaching, movements, even if a loosely somatotopic gradient in preference may exist for hand versus arm movements.

Moreover, discriminative information was contained not only in the most important voxels, but in the least important voxels as well. Neither the top (e.g., 10%) discriminating voxels nor the least discriminating voxels were clustered in particular anatomical regions. While univariate fMRI analyses tend to focus on the most significant activations correlated with one condition, action-related representations can still be discriminated based on distributed patterns of less differential activation with MVPA. This result also argues against a localized representation of action observation and execution, in contrast to traditional univariate fMRI analyses that set high cutoff thresholds and use stringent corrections for multiple comparisons, thus giving the

illusion of isolated, modular activations. Previous MVPA studies have analyzed patterns of activity related to observation of different hand actions in small regions of interest, such as the human homolog of AIP and PMv (Ogawa and Inui 2010). Our results show distributed action-related representations beyond these traditional regions of interest. The large number of cortical areas that participate in sensorimotor matching between visual and motor aspects of actions is also consistent with other recent reports of widely distributed multisensory responses throughout neocortex (Ghazanfar and Schroeder 2006).

Distinct Activation Exists Within Commonly Activated Regions

Previous univariate fMRI studies have identified commonly activated areas that respond to action observation, execution, and mental simulation (Grèzes and Decety 2001), without being able to address how predictive different regions (mirror neuron vs. nonmirror-neuron) are of individual conditions. It has been proposed that the brain represents observed actions by activating mental simulation networks, whereby we mentally simulate an observed action using largely the same neural substrates we would use to produce the same action (Jeannerod 1994; Evangeliou et al. 2009; Savaki 2010).

A mechanism that involves mapping observed actions onto one's own motor system raises the question of how we are able to distinguish between our own actions and other people's actions, and between our imagined and executed actions. One obvious explanation is that there are differences in the magnitude (or presence vs. absence) of activation in primary motor, somatosensory, and other areas that distinguish actual movement from observation of movement. For instance, whereas Broca's area shows equal MEG response amplitudes for observation and execution of hand actions, left and right M1 show stronger responses to execution than observation (Nishitani and Hari 2000). Similarly, there are differences in visual stimulation during observation or execution of movement versus motor imagery (e.g., see Filimon et al. 2007). It has also been suggested that action observation could be accompanied by inhibition of cell firing, thereby also signaling a self-other distinction (Mukamel et al. 2010). This could include inhibition in pyramidal tract neurons of premotor area F5 (Kraskov et al. 2009), in addition to inhibition in M1 (Vigneswaran et al. 2013). It has also been shown that there is a decrease of glucose consumption in the spinal cord forelimb representation during action observation in macaques (Stamos et al. 2010).

Our results show that while observation, execution, and mental simulation of reaching overlap in premotor and posterior parietal cortices, patterns of activation within these commonly activated areas are actually distinct, even in cases where univariate analyses have failed to reveal differences in amount of BOLD activation between conditions at the group level (Filimon et al. 2007). These findings suggest that the brain could distinguish between observation, execution, and mental simulation not just based on whether or not additional areas are recruited for individual conditions, but also based on the pattern of information *within* commonly activated areas in the action observation and simulation network.

Action-Related Information Exists in Both Posterior Parietal and Premotor Cortex

Interestingly, there was no difference in classifier performance based on premotor versus posterior parietal activations. The question of how "motor" the PPC is compared with frontal motor regions remains debated (for reviews, see Goldberg et al. 2006; Andersen and Cui 2009; Filimon 2010; Medendorp et al. 2011; see also Johnson et al. 1996; Mattingley et al. 1998). Based on direct projections from caudal PMd to M1 and the spinal cord, which the PPC does not have, one might have predicted greater discrimination performance for executed reaching versus the other conditions in the premotor than the PPC ROI, especially in the anatomical ROIs. However, our results show that discrimination of executed reaching from the other conditions was as high using premotor ROIs as it was using posterior parietal ROIs, both for anatomical and overlap ROIs. The direction of information flow during motor control, e.g., from frontal to parietal areas or vice versa, appears to depend on the task and the specific parieto-frontal circuit (Filimon 2010). Based on our MVPA results, either frontal or parietal regions can be informative for decoding reaching movements. This has implications for neural prostheses and brain–machine interfaces for movement-impaired populations. If frontal motor areas were damaged due to stroke or degeneration, the distributed nature of movement-related information might allow decoding of motor goals from parietal regions alone. Studies on macaques have already demonstrated the feasibility of neural prosthetics based on PPC activity (Anderson and Cui 2009). In macaques, decoding accuracies improve if larger neuronal ensembles are used, except if a small subset of highly tuned (i.e., most predictive) neurons are selected for decoding, consistent with our MVPA results of a small set of most-predictive voxels being sufficient (Lebedev et al. 2008). This has led to the suggestion that decoding multiple areas simultaneously, including regions less tuned to specific movement parameters, could improve the performance of brain–machine interfaces, with information being accessible from almost any part of the distributed network (Lebedev et al. 2008).

We also examined discriminability between observation, imagery, and execution of reaching in OT cortex. While all 3 conditions could indeed be discriminated with very high accuracy in the ROI as a whole, imagined reaching led to much weaker activations in most of OT, consistent with previous findings of weak or nonsignificant motor imagery activations in most of OT (Astafiev et al. 2004; Filimon et al. 2007; Orlov et al. 2010). [14C]-deoxyglucose mapping in macaque visual areas along occipitotemporal cortex (macaque V3d and V3A) has shown activations for reaching to grasp both in the dark and in light, as well as for observation of reaching to grasp (Kilintari et al. 2011). Specifically, occipitoparietal portions of macaque V3d were more active during action execution in the dark than in light, suggesting recruitment of stored visual representations, or mental imagery. Occipitotemporal parts of V3d were more active for reaching to grasp in the light. This is consistent with our MVPA results in OT: anterior and superior (occipitoparietal) parts of OT showed positive evidence for motor imagery (and execution), whereas the largest, inferior parts showed positive evidence for action observation. It is possible that OT is primarily driven by visual information related to mental simulation (Kilintari et al. 2011).

Are These Mirror Neurons or Sensorimotor Neurons Involved in Motor Preparation?

In this study, we are not attempting to resolve the debate surrounding the contribution of mirror neurons to action

understanding (Hickok 2009). Our results show that information about action is distributed and extends beyond Broca's area, PMv, and the IPL, with no particular clustering of informative voxels in dorsal versus ventral areas or vice versa. Thus, any claim that observed actions are "understood" predominantly based on activity in a mirror neuron network consisting of Broca's area/PMv and the IPL alone would have to account for the widespread activations we report here, and propose a model for how fronto-parietal activations outside and within Broca's area/PMv and the IPL are integrated (for a critique, see also Savaki 2010). If one were to assume that "true" or "core" mirror neuron areas for hand actions consist of only Broca's/PMv and IPL (not including areas outside parietal and frontal cortex, such as the superior temporal sulcus), it is unclear why there would be large areas outside Broca's/PMv and IPL that are also activated by both action execution and action observation, and yet have nothing to do with matching observed and executed actions. Our results are compatible with an interpretation of mirror neurons existing in multiple premotor and posterior parietal areas, as well as with an interpretation of observed and executed actions being matched due to mental simulation in regular sensorimotor neurons that are not mirror neurons per se (Savaki 2010). As argued by Hickok (2009), whether mirror neurons are special neurons as opposed to sensorimotor neurons involved in action representation remains to be addressed using single-cell recordings that could further characterize the functional characteristics of these neurons.

It has been proposed to use selectivity for different observed and executed movements (Dinstein et al. 2008), or discriminability between slightly different observed movements (Oosterhof et al. 2010), as an index of mirror neuron activity. However, the majority of mirror neurons are not strictly congruent, but broadly congruent, that is, the majority of mirror neurons respond similarly to different movements as long as the goal is the same (Rizzolatti et al. 2001). In fact, many mirror neurons in area F5 fire regardless of whether an action is performed with the left hand, right hand, or the mouth (Rizzolatti and Fabbri-Destro 2008). This suggests that requiring "mirror neuron voxels" to discriminate between different specific hand actions, or to show act-specific overlap between observation and execution (Lingnau et al. 2009) will effectively exclude large areas of possible mirror neuron activations. This is why we opted for mapping the information content of dorsal and ventral voxels across observation, execution, and motor imagery here, with the lack of concentration of discriminating voxels in either ventral or dorsal areas suggesting that traditional mirror neuron areas contain neither more nor less information about observed action than nonmirror-neuron areas. Our approach is thus complementary to decoding approaches that emphasize discriminability between movements.

It has been suggested that since dorsal premotor and superior parietal neurons are involved in motor preparation, they should not be considered proper mirror neurons (Rizzolatti and Sinigaglia 2010). However, excluding neurons based on their involvement in motor preparation contradicts the idea that the MNS maps observed actions onto the same motor network that is recruited "when the observer plans their own actions" (Rizzolatti and Sinigaglia 2010, p. 268). Other mental simulation proponents have explicitly argued for an activation of motor preparatory and planning circuits during action observation as the basis of the representation of the observed action (Jeannerod 1994). Arguing against a motor preparatory involvement for mirror neurons also contradicts evidence from TMS that shows motor facilitation from action observation even in muscles (Fadiga et al. 1995), which is precisely taken to be indicative of the mirror neuron circuit (Rizzolatti and Sinigaglia 2010). It is unclear why some sensorimotor areas are considered to be part of the parieto-frontal MNS, such as areas LIP and VIP, while others are arbitrarily excluded, such as PMd and SPL (Rizzolatti and Sinigaglia 2010; see Hickok 2009, for a discussion of motor preparation and mirror neurons; see also Savaki (2010), for a critique of MNS exclusion criteria).

Do Different Patterns of Activation Across Voxels in Regions of Overlapping Activations Imply Separate Neuronal Populations?

Our results show that there are different patterns of activation associated with different conditions even within the overlap ROIs selected in PMd and the SPL/intraparietal cortex. The overlap ROIs consisted of contiguous voxels, all of which were significantly activated above baseline ($P < 0.001$, see Materials and Methods) by all 3 conditions. The MVPA results show that even within these areas of overlapping functional activations, where univariate analyses revealed that all voxels participated in all 3 conditions, the pattern of activation across voxels was sufficiently different to discriminate between execution, observation, and imagery of reaching. This is consistent with successful attempts at decoding overlapping activations using MVPA in extrastriate cortex (Peelen et al. 2006). Critically, the different patterns of activation across commonly activated voxels do not necessarily imply separate neuronal populations within voxels that are active in different conditions (e.g., Peelen and Downing 2007). The separable MVPA patterns could also be due to neurons responding to multiple stimuli with different levels of activation. Thus the same neurons could be active for all conditions—but to different degrees and while synchronizing in different sub-networks. Functional MRI does not have the spatial resolution to determine whether separate populations of neurons are leading to the activation of a single voxel in different conditions. Whether this signal is due to neuronal population A being active during condition X, and spatially interleaved population B being active during condition Y, or the same population of neurons being active in both conditions, is impossible to tell. MVPA does not change this fact, even if different patterns are found across distributed voxels. Although we cannot know for certain, the result that observation, execution, and imagery of actions led to large, continuous swaths of activations across contiguous voxels (see black outline of the overlap ROIs in Fig. 4 and Filimon et al. 2007), and the tendency of neurons with similar functionality to cluster together, suggest that the fine-grained patterns of discriminating weights across commonly activated voxels are due to the same neurons being involved in all conditions, albeit to varying degrees and forming different sub-networks. The large overlaps between observation, execution, and imagery are unlikely to be due to neuronal populations that are separate within each voxel across the entire swath of commonly activated voxels, that is, due to a mosaic of separate observation, execution, and imagery populations repeated across all the voxels forming the area of functional overlap.

Future Research Directions

Future fMRI research could address whether there is increased functional connectivity between different sub-regions within

PPC or premotor cortex, or between posterior parietal and premotor sub-regions. For instance, using event-related fMRI designs, voxels shown by MVPA to participate in different distributed patterns underlying observation and execution could be used as seed voxels in a functional connectivity analysis. If the functional connectivity between voxels that are commonly activated by multiple conditions changes across conditions, this could lend support to the idea that functional sub-networks form within the same population of neurons, rather than separate populations participating in individual conditions only.

At the single-unit level, areas outside macaque F5 and IPL need to be tested during observation and execution of more types of nongrasping or nongoal-directed limb actions. It also remains to be shown whether there is a difference between mirror neurons and sensorimotor neurons that participate in movement preparation in addition to action observation and execution. Finally, advances in multi-unit recording techniques and in simultaneous recordings from multiple areas could address whether observation of different movements, especially nongoal-directed movements, also involves widely distributed networks of mirror neurons outside traditional mirror neuron areas F5 and the IPL, as suggested by action observation activations in humans.

Summary

By using MVPA to address questions of motor representations in the human brain, we have shown that multiple distributed patterns of activity in frontal motor and posterior parietal areas underlie observation, execution, and imagery of reaching movements. Action-related information was distributed across both ventral and dorsal areas in both premotor cortex and PPC, rather than solely in traditional mirror neuron regions. Distributed patterns exist even in regions that are commonly activated by all conditions, allowing local distinction between execution, imagery, and observation of action. Finally, posterior parietal and premotor patterns of activity are equally predictive of whether the brain is engaged in reaching, observation of reaching, or reaching imagery.

Funding

C.R. and F.F. were supported by NSF IGERT Grant DGE-0333451 to G.W.C/VR de Sa. G.W.C was supported in part by NSF grants SBE 0542013 and SMA 1041755 to the Temporal Dynamics of Learning Center, an NSF Science of Learning Center.

Notes

We thank 7 anonymous reviewers and Jonathan D. Nelson for their helpful comments on earlier versions of the manuscript. *Conflict of Interest*: None declared.

References

Abdollahi RO, Jastorff J, Orban GA. 2012. Common and segregated processing of observed actions in human SPL. Cereb Cortex. 23 (11):2734–2753.

Andersen RA, Cui H. 2009. Intention, action planning, and decision making in parietal-frontal circuits. Neuron. 63:568–583.

Astafiev SV, Stanley CM, Shulman GL, Corbetta M. 2004. Extrastriate body area in human occipital cortex responds to the performance of motor actions. Nat Neurosci. 7(5):542–548.

Baird AD, Scheffer IE, Wilson SJ. 2011. Mirror neuron system involvement in empathy: a critical look at the evidence. Soc Neurosci. 6 (4):327–335.

Battaglia-Mayer A, Caminiti R, Lacquaniti F, Zago M. 2003. Multiple levels of representation of reaching in the parieto-frontal network. Cereb Cortex. 13:1009–1022.

Battaglia-Mayer A, Ferraina S, Genovesio A, Marconi B, Squatrito S, Lacquaniti F, Caminiti R. 2001. Eye–hand coordination during reaching. II. An analysis of the relationships between visuomanual signals in parietal cortex and parieto-frontal association projections. Cereb Cortex. 11:528–544.

Bracci S, Ietswaart M, Peelen MV, Cavina-Pratesi C. 2010. Dissociable neural responses to hands and non-hand body parts in human left extrastriate visual cortex. J Neurophysiol. 103(6):3389–3397.

Buccino G, Binkofski F, Fink GR, Fadiga L, Fogassi L, Gallese V, Seitz RJ, Zilles K, Rizzolatti G, Freund HJ. 2001. Action observation activates premotor and parietal areas in a somatotopic manner: an fMRI study. Eur J Neurosci. 13(2):400–404.

Burnod Y, Baraduc P, Battaglia-Mayer A, Guignon E, Koechlin E, Ferraina S, Lacquaniti F, Caminiti R. 1999. Parieto-frontal coding of reaching: an integrated framework. Exp Brain Res. 129:325–346.

Caminiti R, Chafee MV, Battaglia-Mayer A, Averbeck BB, Crowe DA, Georgopoulos AP. 2010. Understanding the parietal lobe syndrome from a neurophysiological and evolutionary perspective. Eur J Neurosci. 31:2320–2340.

Carpaneto J, Umilta MA, Fogassi L, Murata A, Gallese V, Micera S, Raos V. 2011. Decoding the activity of grasping neurons recorded from the ventral premotor area F5 of the macaque monkey. Neuroscience. 188:80–94.

Caspers S, Zilles K, Laird AR, Eickhoff SB. 2010. ALE meta-analysis of action observation and imitation in the human brain. NeuroImage. 50(3):1148–1167.

Cavina-Pratesi C, Monaco S, Fattori P, Galletti C, McAdam TD, Quinlan DJ, Goodale MA, Culham JC. 2010. Functional magnetic resonance imaging reveals the neural substrates of arm transport and grip formation in reach-to-grasp actions in humans. J Neurosci. 30(31):10306–10323.

Cisek P, Kalaska JF. 2002. Simultaneous encoding of multiple potential reach directions in dorsal premotor cortex. J Neurophysiol. 87 (2):1149–1154.

Cross ES, Kraemer DJM, Hamilton AFDC, Kelley WM, Grafton ST. 2009. Sensitivity of the action observation network to physical and observational learning. Cereb Cortex. 19(2):315–326.

Culham JC, Cavina-Pratesi C, Singhal A. 2006. The role of parietal cortex in visuomotor control: What have we learned from neuroimaging? Neuropsychologia. 44:2668–2684.

Culham JC, Valyear KF. 2006. Human parietal cortex in action. Curr Opin Neurobiol. 16:205–212.

Dale AM, Fischl B, Sereno MI. 1999. Cortical surface-based analysis. I. Segmentation and surface reconstruction. NeuroImage. 9:179–194.

Decety J. 2010. To what extent is the experience of empathy mediated by shared neural circuits? Emot Rev. 2(3):204–207.

Destrieux C, Fischl B, Dale A, Halgren E. 2010. Automatic parcellation of human cortical gyri and sulci using standard anatomical nomenclature. NeuroImage. 53:1–15.

Dinstein I, Thomas C, Behrmann M, Heeger DJ. 2008. A mirror up to nature. Curr Biol. 18:R13–R18.

di Pellegrino G, Fadiga L, Fogassi L, Gallese V, Rizzolatti G. 1992. Understanding motor events: a neurophysiological study. Exp Brain Res. 91(1):176–180.

Dushanova J, Donoghue J. 2010. Neurons in primary motor cortex engaged during action observation. Eur J Neurosci. 31(2):386–398.

Evangeliou MN, Raos V, Galletti C, Savaki HE. 2009. Functional imaging of the parietal cortex during action execution and observation. Cereb Cortex. 19(3):624–639.

Fadiga L, Fogassi L, Pavesi G, Rizzolatti G. 1995. Motor facilitation during action observation: a magnetic stimulation study. J Neurophysiol. 73(6):2608–2611.

Fattori P, Breveglieri R, Marzocchi N, Filippini D, Bosco A, Galletti C. 2009. Hand orientation during reach-to-grasp movements modulates neuronal activity in the medial posterior parietal area V6A. J Neurosci. 29:1928–1936.

Fattori P, Raos V, Breveglieri R, Bosco A, Marzocchi N, Galletti C. 2010. The dorsomedial pathway is not just for reaching: grasping neurons in the medial parieto-occipital cortex of the macaque monkey. J Neurosci. 30:342–349.
Ferrari PF, Rozzi S, Fogassi L. 2005. Mirror neurons responding to observation of actions made with tools in monkey ventral premotor cortex. J Cog Neurosci. 17:212–226.
Filimon F. 2010. Human cortical control of hand movements: parietofrontal networks for reaching, grasping, and pointing. Neuroscientist. 16(4):388–407.
Filimon F, Nelson JD, Hagler DJ, Sereno MI. 2007. Human cortical representations for reaching: mirror neurons for execution, observation, and imagery. NeuroImage. 37(4):1315–1328.
Filimon F, Nelson JD, Huang RS, Sereno MI. 2009. Multiple parietal reach regions in humans: cortical representations for visual and proprioceptive feedback during on-line reaching. J Neurosci. 29 (9):2961–2971.
Filimon F, Philiastides MG, Nelson JD, Kloosterman NA, Heekeren HR. 2013. How embodied is perceptual decision making?—Evidence for separate processing of perceptual and motor decisions. J Neurosci. 33(5):2121–2136.
Fischl B, Sereno MI, Dale AM. 1999. Cortical surface-based analysis. II: Inflation, flattening, and a surface-based coordinate system. NeuroImage. 9:195–207.
Fogassi L, Ferrari PF. 2011. Mirror systems. Wiley Interdiscip Rev Cogn Sci. 2:22–38.
Fogassi L, Ferrari PF, Gesierich B, Rozzi S, Chersi F, Rizzolatti G. 2005. Parietal lobe: from action organization to intention understanding. Science. 308(5722):662–667.
Gallese V, Fadiga L, Fogassi L. 1996. Action recognition in the premotor cortex. Brain. 119(2):593–609.
Gallivan JP, Cavina-Pratesi C, Culham JC. 2009. Is that within reach? fMRI reveals that the human superior parieto-occipital cortex (SPOC) encodes objects reachable by the hand. J Neurosci. 29 (14):4381–4391.
Gallivan JP, McLean DA, Smith FW, Culham JC. 2011. Decoding effector-dependent and effector-independent movement intentions from human parieto-frontal brain activity. J Neurosci. 31 (47):17149–17168.
Gamberini M, Galletti C, Bosco A, Breveglieri R, Fattori P. 2011. Is the medial posterior parietal area V6A a single functional area? J Neurosci. 31:5145–5157.
Gentilucci M, Fogassi L, Luppino G, Matelli M, Camarda R, Rizzolatti G. 1988. Functional organization of inferior area 6 in the macaque monkey. Exp Brain Res. 71:491–507.
Ghazanfar A, Schroeder CE. 2006. Is neocortex essentially multisensory? Trends Cogn Sci. 10:278–285.
Goldberg ME, Bisley JW, Powell KD, Gottlieb J. 2006. Saccades, salience and attention: the role of the lateral intraparietal area in visual behavior. Prog Brain Res. 155:157–175.
Grafton ST. 2009. Embodied cognition and the simulation of action to understand others. Ann N Y Acad Sci. 1156:97–117.
Gregoriou GG, Luppino G, Matelli M, Savaki HE. 2005. Frontal cortical areas of the monkey brain engaged in reaching behavior:A14 C–deoxyglucose imaging study. Neuroimage. 27:442–464.
Gregoriou GG, Savaki HE. 2003. When vision guides movement: a functional imaging study of the monkey brain. Neuroimage. 19:959–967.
Grèzes J, Decety J. 2001. Functional anatomy of execution, mental simulation, observation, and verb generation of actions: a meta-analysis. Hum Brain Mapp. 12(1):1–19.
Guyon I, Weston J, Barnhill S, Vapnik V. 2002. Gene selection for cancer classification using support vector machines. Mach Learn. 46(1):389–422.
Hagler DJ Jr, Saygin AP, Sereno MI. 2006. Smoothing and cluster thresholding for cortical surface-based group analysis of fMRI data. NeuroImage. 33(4):1093–1103.
Hanson SJ, Halchenko YO. 2008. Brain reading using full brain support vector machines for object recognition: there is no "face" identification area. Neural Comput. 20(2):486–503.
Heed T, Beurze SM, Toni I, Röder B, Medendorp WP. 2011. Functional rather than effector-specific organization of human posterior parietal cortex. J Neurosci. 31(8):3066–3076.
Hickok G. 2009. Eight problems for the mirror neuron theory of action understanding in monkeys and humans. J Cog Neurosci. 21(7):1229–1243.
Hickok G, Hauser M. 2010. (Mis)understanding mirror neurons. Curr Biol. 20(14):593–594.
Holm S. 1979. A simple sequentially rejective multiple test procedure. Scand J Stat. 6:65–70.
Jastorff J, Begliomini C, Fabbri-Destro M, Rizzolatti G, Orban GA. 2010. Coding observed motor acts: different organizational principles in the parietal and premotor cortex of humans. J Neurophysiol. 104 (1):128–140.
Jeannerod M. 1994. The representing brain: neural correlates of motor intention and imagery. Behav Brain Sci. 17(2):187–245.
Joachims T. 1999. Making large-scale support vector machine learning practical. In: Schölkopf B, Burges CJ, Smola AJ, editors. Advances in kernel methods: support vector learning. Cambridge, MA: MIT Press. p. 169–184.
Johnson PB, Ferraina S, Bianchi L, Caminiti R. 1996. Cortical networks for visual reaching: physiological and anatomical organization of frontal and parietal lobe arm regions. Cereb Cortex. 6: 102–119.
Kaas JH. 2012. Evolution of columns, modules, and domains in the neocortex of primates. Proc Natl Acad Sci. 109:10655–10660.
Kaas JH, Gharbawie OA, Stepniewska I. 2011. The organization and evolution of dorsal stream multisensory motor pathways in primates. Front Neuroanat. 5(34):1–7.
Keysers C, Gazzola V. 2009. Expanding the mirror: vicarious activity for actions, emotions, and sensations. Curr Opin Neurobiol. 19:666–671.
Kilintari M, Raos V, Savaki HE. 2011. Grasping in the dark activates early visual cortices. Cereb Cortex. 21:949–963.
Kraskov A, Dancause N, Quallo MM, Shepherd S, Lemon RN. 2009. Corticospinal neurons in macaque ventral premotor cortex with mirror properties: a potential mechanism for action suppression? Neuron. 64:922–930.
Lebedev MA, O'doherty JE, Nicolelis MA. 2008. Decoding of temporal intervals from cortical ensemble activity. J Neurophysiol. 99:166–186.
Lingnau A, Gesierich B, Caramazza A. 2009. Asymmetric fMRI adaptation reveals no evidence for mirror neurons in humans. Proc Natl Acad Sci. 106(24):9925–9930.
Mattingley JB, Husain M, Rorden C, Kennard C, Driver J. 1998. Motor role of human inferior parietal lobe revealed in unilateral neglect patients. Nature. 392:179–182.
Medendorp WP, Buchholz VN, Van Der Werf J, Leoné FT. 2011. Parietofrontal circuits in goal-oriented behaviour. Eur J Neurosci. 33:2017–2027.
Medendorp WP, Goltz HC, Crawford JD, Vilis T. 2005. Integration of target and effector information in human posterior parietal cortex for the planning of action. J Neurophysiol. 93(2):954–962.
Molenberghs P, Cunnington R, Mattingley JB. 2012. Brain regions with mirror properties: a meta-analysis of 125 human fMRI studies. Neurosci Biobehav Rev. 36(1):341–349.
Molenberghs P, Cunnington R, Mattingley JB. 2009. Is the mirror neuron system involved in imitation? A short review and meta-analysis. Neurosci Biobehav Rev. 33(7):975–980.
Monaco S, Cavina-Pratesi C, Sedda A, Fattori P, Galletti C, Culham JC. 2011. Functional magnetic resonance adaptation reveals the involvement of the dorsomedial stream in hand orientation for grasping. J Neurophysiol. 106(5):2248–2263.
Morin O, Grèzes J. 2008. What is "mirror" in the premotor cortex? A review. Clin Neurophysiol. 38(3):189–195.
Mukamel R, Ekstrom AD, Kaplan J, Iacoboni M, Fried I. 2010. Single-neuron responses in humans during execution and observation of actions. Curr Biol. 20(8):750–756.
Nishitani N, Hari R. 2000. Temporal dynamics of cortical representation for action. Proc Natl Acad Sci. 97(2):913–918.
Norman KA, Polyn SM, Detre GJ, Haxby JV. 2006. Beyond mind-reading: multi-voxel pattern analysis of fMRI data. Trends Cogn Sci. 10(9):424–430.
Ogawa K, Inui T. 2010. Neural representation of observed actions in the parietal and premotor cortex. NeuroImage. 56(2):728–735.
Oosterhof NN, Wiggett AJ, Diedrichsen J, Tipper SP, Downing PE. 2010. Surface-based information mapping reveals crossmodal

vision-action representations in human parietal and occipitotemporal cortex. J Neurophysiol. 104(2):1077–1089.
Orlov T, Makin TR, Zohary E. 2010. Topographic representation of the human body in the occipitotemporal cortex. Neuron. 68(3):586–600.
Peelen MV, Downing PE. 2007. Using multi-voxel pattern analysis of fMRI data to interpret overlapping functional activations. Trends Cogn Sci. 11(1):424–430.
Peelen MV, Wiggett AJ, Downing PE. 2006. Patterns of fMRI activity dissociate overlapping functional brain areas that respond to biological motion. Neuron. 49(6):815–822.
Pitzalis S, Sereno MI, Committeri G, Fattori P, Galati G, Tosoni A, Galletti C. 2013. The human homologue of macaque area V6A. Neuroimage. 82C:517–530.
Ramsey R, de C Hamilton AF. 2010. Understanding actors and object-goals in the human brain. Neuroimage. 50(3):1142–1147.
Raos V, Evangeliou MN, Savaki HE. 2007. Mental simulation of action in the service of action perception. J Neurosci. 27(46):12675–12683.
Raos V, Evangeliou MN, Savaki HE. 2004a. Observation of action: grasping with the mind's hand. NeuroImage. 23(1):193–201.
Raos V, Franchi G, Gallese V, Fogassi L. 2003. Somatotopic organization of the lateral part of area F2 (dorsal premotor cortex) of the macaque monkey. J Neurophysiol. 89:1503–1518.
Raos V, Kilintari M, Savaki HE. 2014. Viewing a forelimb induces widespread cortical activations. NeuroImage. 89:122–142.
Raos V, Umiltá MA, Gallese V, Fogassi L. 2004b. Functional properties of grasping-related neurons in the dorsal premotor area F2 of the macaque monkey. J Neurophysiol. 92:1990–2002.
Rizzolatti G, Fabbri-Destro M. 2008. The mirror system and its role in social cognition. Curr Opin Neurobiol. 18(2):179–184.
Rizzolatti G, Fadiga L, Gallese V, Fogassi L. 1996. Premotor cortex and the recognition of motor actions. Cogn Brain Res. 3(2):131–141.
Rizzolatti G, Fogassi L, Gallese V. 2001. Neurophysiological mechanisms underlying the understanding and imitation of action. Nat Rev Neurosci. 2:661–670.
Rizzolatti G, Sinigaglia C. 2010. The functional role of the parieto-frontal mirror circuit: interpretations and misinterpretations. Nat Rev Neurosci. 11(4):264–274.
Sakreida K, Schubotz RI, Wolfensteller U, Von Cramon DY. 2005. Motion class dependency in observers' motor areas revealed by functional magnetic resonance imaging. J Neurosci. 25(6):1335–1342.
Savaki HE. 2010. How do we understand the actions of others? By mental simulation, NOT mirroring. Cogn Critique. 2:99–140.
Stamos AV, Savaki HE, Raos V. 2010. The spinal substrate of the suppression of action during action observation. J Neurosci. 30 (35):11605–11611.
Tkach D, Reimer J, Hatsopoulos NG. 2007. Congruent activity during action and action observation in motor cortex. J Neurosci. 27 (48):13241–13250.
Valyear KF, Culham JC. 2010. Observing learned object-specific functional grasps preferentially activates the ventral stream. J Cogn Neurosci. 22(5):970–984.
Vigneswaran G, Philipp R, Lemon RN, Kraskov A. 2013. M1 corticospinal mirror neurons and their role in movement suppression during action observation. Curr Biol. 23(3):236–243.